

Relation between Coal and Fly Ash Mineralogy, Based on Quantitative X-Ray Diffraction Methods

Colin R. Ward¹ and David French²

Co-operative Research Centre for Coal in Sustainable Development: ¹School of Biological, Earth and Environmental Sciences, University of New South Wales, Sydney 2052, Australia; ²CSIRO Division of Energy Technology, Lucas Heights Advanced Technology Centre, PMB 7, Menai 2234, Australia.

KEYWORDS: mineralogy, coal, fly ash, quantitative X-ray diffraction

ABSTRACT

The proportion of amorphous or glassy material in a series of fly ashes has been evaluated by X-ray powder diffraction (XRD) using several different sample preparation and processing methods in conjunction with the Rietveld-based Siroquant quantitative X-ray diffraction analysis software package. The results of the different methods used were found to give consistent results and were also in agreement with published data for a reference fly ash sample.

Comparison to the mineral matter in the respective feed coals showed that the relative proportions of quartz in the LTA of the feed coal and in the fly ash are strongly correlated to each other, suggesting that much of the quartz in the coal tends to pass directly into the fly ash, without significant alteration. A similar comparison for the iron minerals in the coal and fly ash shows a more scattered but still broadly linear relationship between the percentage of iron oxide minerals in the fly ash and the percentage of siderite plus pyrite in the LTA of the corresponding feed coal, suggesting that the iron oxide minerals in the fly ash are derived mainly from the iron minerals present in the coals themselves.

Calculations based on subtracting the inferred chemistry of the crystalline minerals in the fly ashes from the total fly ash chemistry were also used to estimate the overall chemical composition of the glass fraction in the fly ashes and show that ashes derived from lower-rank coals have different glass compositions to those derived from higher-rank (bituminous) materials.

INTRODUCTION

Fly ash can be regarded for many purposes as containing three different types of constituents: crystalline minerals (quartz, mullite, spinel etc), unburnt carbon particles, and non-crystalline aluminosilicate glass. Examination under the optical and electron microscope typically shows that, although crystal fragments and crystalline aggregates may be more abundant in some fly ashes than others, and different types of unburnt carbon particles can also be significant constituents, most of the ash is typically made up of glassy material. Glass is also present to a varying extent in slags and other combustion by-products.

Because of its poorly ordered atomic structure, porous nature and overall abundance, the glass is usually the main constituent involved in chemical reactions associated with ash utilisation, such as in the cement and concrete industry, or in geopolymer and zeolite production. The glass also appears to be a major host within the ash for adsorbed trace elements, which may be loosely held to the glass surfaces and thus have significant potential for release into the surrounding environment. Glass in natural volcanic rocks is relatively unstable during chemical weathering, and glass in coal ash may also be expected to break down with prolonged exposure, a process that may further release elements into surrounding environmental systems.

For these and other reasons it is desirable to assess not only the overall or bulk chemistry in fly ash characterisation, but also the relative abundance of the different mineralogical constituents, including the glassy material, and, if possible, the chemical composition of the glass component within the ash as well. Such information helps to compare and contrast individual ashes with each other, leading possibly to more precise ash classifications. It is also of great value in better relating the characteristics of the ash to those of the parent coals, as a basis for understanding the processes associated with ash formation, and perhaps providing a more scientific basis for controlling the selection and quality of ash materials for use in different applications.

MINERALOGICAL ANALYSIS TECHNIQUES

Volumetric estimates of the abundance of different constituents are routinely made for coals and other rocks under the microscope using point-count techniques [1]. Although this technique may also be used in fly ash studies [2, 3], the crystalline components in fly ash are commonly too small, and too intimately inter-grown with the glass, to allow definitive mineral identification, or to provide reliable estimates of the proportions of the different mineral and glass phases in ash samples by microscopic methods. Microscope techniques can nevertheless provide useful information on the size and shape of the individual particles in a fly ash sample, and of the mode of occurrence of the principal crystalline components. They are of particular value in the study of unburnt carbon particles, where the textures revealed under the microscope are used to identify the different types of carbonaceous material present [4].

X-ray diffraction (XRD) has long been used as a definitive technique for identification of crystalline mineral components [5], and represents the most suitable method for identifying minerals and other crystalline phases in a wide range of natural and synthetic materials. XRD is especially useful in materials such as fly ash, where the individual crystals are too small to be reliably identified by other techniques. However, glass is effectively amorphous or non-crystalline, and does not have regular arrays of atoms that produce definitive peaks in X-ray diffraction studies. Broad patterns or “humps” may nevertheless be seen in X-ray diffractograms derived from different types of glassy materials. Along with an overall reduction in the peak intensities derived from the crystalline components, due to dilution and/or mass absorption effects, these humps provide an indication that glass is present in fly ashes and other samples subjected to XRD analysis.

QUANTITATIVE X-RAY DIFFRACTION METHODS

Although X-ray diffraction provides an almost unequivocal basis for mineral identification, it has traditionally been thought to have limitations in determining mineral proportions (i.e. as a tool for quantitative analysis) due to factors such as the inherent variability of some crystal structures, grain size effects, preferred orientation, and the absorption of X-rays by other components in the mixture. Several methods have nevertheless been developed to counteract some of these effects [6]. These include techniques based on spiking the powdered sample with a known mass of an easily identified mineral not otherwise present (typically fluorite or corundum), and evaluating the ratio of a key peak intensity for each mineral to the intensity of a key peak derived from the spike component [7, 8]. Such methods, however, require a separate series of calibration experiments based on relatively pure mineral standards, and are also inherently limited to evaluation of only a small number of minerals in a multi-component mixture.

The value of XRD as a quantitative tool has, however, been enhanced in recent years following development of computer processing systems based on the principles of full-profile diffractogram analysis developed by Rietveld [9]. One of these is the Siroquant technique, developed in Australia by CSIRO [10]. The Siroquant processing system uses fundamental data on mineral structure to generate a synthetic XRD pattern that can be systematically adjusted through a user-friendly interface to match the observed XRD pattern of the sample under analysis [11]. The scaling factors developed in this process are then used to evaluate the percentages of the different crystalline phases or minerals present.

Up to 25 different minerals can be incorporated in a routine Siroquant analysis. Allowance is made during the process for factors such as crystal lattice variations, preferred orientation, diffraction peak profile, and differential absorption of diffracted X-rays by other minerals in the mixture. Because of its ease of operation and the wide range of minerals that can be incorporated, the technique represents a considerable advance on methods based on measurement of key peak heights on the diffractogram in relation to the peak heights generated from a known mass of added spiking material. As well as computation of standard XRD patterns from crystallographic and chemical data, reference patterns have also been developed for use in Siroquant directly from measured XRD traces of the mineral in question [12, 13]. These allow phases having imperfectly known or poorly developed crystal structures to be incorporated in the analysis, with data derived from the measured patterns refined and quantified along with those for the other reference components using Rietveld processing methods. Such a capability is particularly relevant to the clay minerals, but is also of potential use in evaluation of glassy components.

The mineral percentages provided by X-ray diffraction and Siroquant, including materials containing clay minerals and similar poorly crystalline components, have been tested for coals and other rocks against independent data derived from chemical analysis [11, 14-17]. The (inferred) chemical composition of the mineral mixture indicated by Siroquant in such cases is usually very close to the (actual) chemical composition of the same material, suggesting a high level of consistency and increasing confidence in the results obtained from using the technique.

As well as determining the relative proportions of crystalline phases, Siroquant and other Rietveld systems have the capacity to determine the proportion of amorphous or non-crystalline material present. This is based on evaluation of a diffractogram of the powdered sample to which a known proportion of a crystalline spike material has been added. The proportion of the spike, along with the other crystalline components, is determined by routine Rietveld processing of the spiked XRD trace. As with other analyses, the proportion of all the crystalline phases, including the spike, is automatically normalised by Siroquant to 100%. If a significant proportion of amorphous material is present in the sample, the proportion of the spike component in this normalised estimate will be higher than the proportion originally weighed in, since the amorphous material is not included with the crystalline phases measured by this part of the Rietveld analysis process. A routine within the Siroquant system can then be used to calculate the proportion of amorphous material in the sample, without the spike component, using a correction based on the weighed-in proportion of the spike added prior to the XRD run. This provides a useful basis for more complete evaluation of fly ash mineralogy, as well as the mineralogy of slags and other combustion by-products, using Rietveld-based XRD techniques.

USE OF SIROQUANT IN FLY ASH STUDIES

The present paper describes the use of X-ray diffraction data and Siroquant processing as a basis for determining the percentage of both the crystalline and the non-crystalline (amorphous or glassy) phases in fly ash samples from a number of different Australian power stations. Fly ashes from a total of nine Australian power stations were evaluated, along with a sample of NIST Fly Ash 1633b, an international reference material distributed by the US National Institute of Standards and Technology. The Australian fly ash samples had been subjected to chemical analysis and other evaluations in a separate study by Killingley et al. [18]. In addition to the certified data on its chemical composition, information on the mineralogy and glass content of NIST 1633b has also been reported separately from XRD studies using another Rietveld-based process by Winburn et al. [19].

An accurately weighed-in spike, amounting to around 15% by weight of each individual fly ash sample, was added to each ground fly ash prior to XRD analysis. Two different spiking materials were used: a synthetic corundum powder and a crystalline zinc oxide. The ash and spike in each case were thoroughly mixed by grinding the spiked samples in an agate pestle and mortar until a homogeneous colour and texture was obtained.

An alternative procedure was also investigated, involving use of XRD data on a poorly crystalline silicate material in the Siroquant database to represent the glass component, and processing the diffractogram of the raw (i.e. unspiked) fly ash sample through Siroquant with this phase included as part of the analysis task. Two different phases were used to represent the glassy material in this type of analysis, a metakaolin pattern and a tridymite pattern, both based on data files prepared independently from observed XRD traces as part of the Siroquant development process [12]. If successful, this would allow quantitative XRD analysis of glass-bearing ash samples without the need for the spiking process.

DETERMINATION OF GLASS CONTENT

The fly ash samples were finely powdered by grinding in a pestle and mortar, and each powder was subjected to XRD analysis using a Philips X'pert diffractometer system with Cu K α radiation. Scans were run from 2 to 60° 2 θ , with increments of 0.04° and a counting time of 2 seconds per step. A typical diffractogram of the raw fly ash obtained from this study is shown in Figure 1. Diffractograms of each fly ash, spiked separately with around 15% (weighed accurately) of synthetic corundum and ZnO, were also obtained for each sample using the same operating conditions.

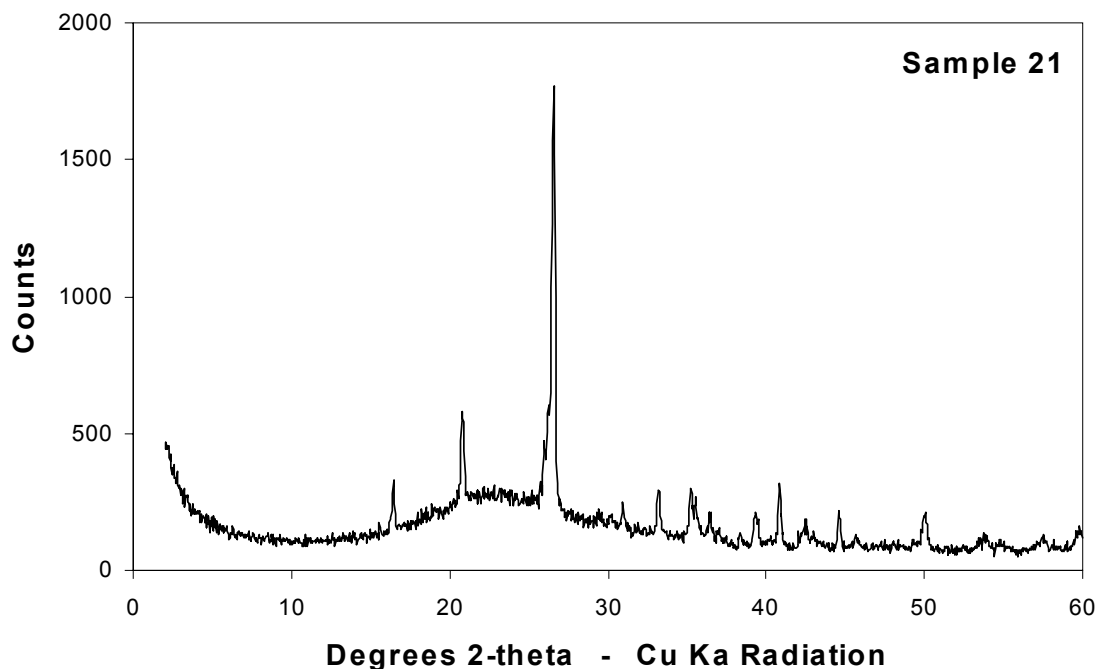


Figure 1: X-ray diffractogram of a typical Australian fly ash

The diffractograms of the spiked and unspiked samples were processed using Siroquant, with results as indicated in Tables 1 and 2. Four sets of results are presented in these tables for each sample. Two of these are based on analysis of samples respectively spiked with corundum and ZnO, with a calculation based on the proportion of weighed-in spike being used to determine the proportion of amorphous material (glass) in each case. The other two are based on analysis of the raw (unspiked) fly ash samples, with either metakaolin or tridymite being incorporated in the analysis task and refined to represent the glass component.

Comparison of the results from the different methods for NIST 1633b (Table 1) shows a good level of agreement for the two spiked patterns and for the raw fly ash pattern using metakaolin to represent the glass fraction. These results are also consistent with data obtained for the same reference sample by Winburn et al. [19] using a different Rietveld-based XRD technique. The data from the raw ash with tridymite included in the analysis task, however, provide a slightly lower “glass” percentage and slightly higher percentages for the various crystalline components.

Similar comparisons for the nine Australian fly ashes (Table 2), with one exception, show a good level of consistency between the results for the two sets of spiked samples. The XRD data for the raw ash samples processed using tridymite to represent the glass fraction also provide similar results. The data for the raw ashes processed using metakaolin, however, show slightly higher “glass” percentages and slightly lower proportions of the major crystalline components.

Table 1: Mineralogical analysis data for NBS Sample 1633b by X-ray diffraction, using different sample preparation and processing techniques

	Corundum spike	ZnO Spike	Metakaolin in task	Tridymite in task	Winburn et al. [19]
Quartz	7.1	7.2	8.1	9.6	6.1
Mullite	22.2	22.5	22.6	27.0	21.8
Magnetite	2.2	2.4	1.6	1.8	3.9
Maghemite	2.0	2.1	2.4	2.8	
Hematite	1.1	0.8	1.2	1.4	2.2
Calcium aluminate	1.1	0.7	1.0	1.1	
Glass	64.3	64.3	63.0	56.3	65.0

Because of the close agreement obtained from use of the two different spike materials, calculation of glass content from the XRD patterns of the spiked samples, using the Siroquant processing system, appears to provide the most consistent and by inference the most reliable mineralogical analysis among the different methods tested. Even though a weighed-in spike is still used, the Siroquant process does not require the separate series of calibration experiments that accompany use of peak intensity ratios in more traditional techniques [6, 7]. Use of a separate mineral phase, such as metakaolin or tridymite, to represent the glass fraction in XRD analysis of raw (unspiked) fly ash, however, also provides acceptable results, with a level of precision that is adequate for many purposes. The present study suggests that metakaolin may provide better consistency with spiked sample results for North American coals (e.g. NIST 1663b), but that tridymite appears to provide better consistency for the Australian fly ash materials.

RELATION TO MINERALS IN FEED COALS

Samples of feed coals associated with seven of the nine ashes were also available for the study. Representative samples of these coals were subjected to ashing at around 120°C in an electronically-excited oxygen plasma [20] using an IPC 4-chamber plasma ashing unit, at 50 watts RF power per chamber, and the weight percentage of low-temperature ash (LTA) determined. The mineralogy of each LTA was also determined by X-ray diffraction and Siroquant (Table 3), and the percentages of the different phases in the coal mineral matter compared to the proportions of relevant phases in the fly ash materials (Figure 2).

Figure 2a shows that the absolute percentage of quartz in the fly ash is less than that in the corresponding LTA, although the relative proportions of quartz in the LTA of the feed coal and in the fly ash appear, with two exceptions (circled), to show a fairly strong correlation to each other. Considered in conjunction with microscopic

observations, which typically show quartz occurring as discrete fragments in the fly ash, this suggests that much of the quartz in the coal tends to pass directly into the fly ash, without significant alteration. The lesser proportion of quartz in the fly ash, however, compared to the coal LTA, suggests that some quartz may become incorporated into the glassy components during ash formation; a small amount may also possibly be lost as a silica fume into the combustion stream. A particularly significant contribution from these processes may also help to explain the less than expected proportion of quartz in the fly ashes represented by the circled data points, compared to the proportion of quartz in the respective coals' mineral matter.

Table 2: Mineralogy of Australian fly ashes by X-ray diffraction and Siroquant using different sample preparation and processing techniques

a) Corundum Spike

Power Station No	15	16	17	18	19	20	21	22	23
Quartz	24.8	3.4	7.6	29.9	26.4	15.9	14.0	8.0	9.3
Mullite	25.6	13.3	13.1	17.4	23.3	29.0	13.4	26.4	14.4
Cristobalite	0.2	0.0	0.0	0.1	0.2	0.1	0.0	0.1	0.1
Magnetite	1.5	2.9	1.0	2.3	0.1	0.0	1.0	1.8	0.0
Maghemite	0.9	1.8	0.4	2.2	0.7	0.8	2.4	0.8	0.8
Hematite	0.7	0.7	0.0	1.4	3.3	0.0	0.2	0.0	0.0
Amorphous = glass	46.3	77.9	77.9	46.7	46.2	54.2	69.0	62.8	75.5

b) ZnO Spike

Power Station No	15	16	17	18	19	20	21	22	23
Quartz	25.4	2.1	7.8	29.8	32.7	12.1	14.1	6.9	9.9
Mullite	24.2	11.9	11.9	18.3	16.5	26.1	15.5	24.5	15.7
Cristobalite	0.1	0.1	0.1	0.1	0.3	0.1	0.1	0.0	0.0
Magnetite	0.8	2.3	0.3	2.5	1.4	0.0	2.5	1.6	0.0
Maghemite	1.2	2.3	0.9	1.5	0.6	0.7	1.5	0.8	0.7
Hematite	0.9	1.4	0.0	1.7	3.5	0.0	0.0	0.1	0.0
Amorphous = glass	47.3	80.0	79.0	46.2	45.1	61.0	66.3	66.0	73.7

c) Metakaolin in Task

Power Station No	15	16	17	18	19	20	21	22	23
Quartz	18.1	2.3	5.2	25.1	26.3	10.0	9.7	5.3	4.9
Mullite	18.5	8.9	8.9	15.2	20.3	21.3	10.2	18.5	8.5
Cristobalite	0.0	0.0	0.1	0.1	0.1	0.0	0.1	0.0	0.0
Magnetite	0.6	1.9	0.0	1.5	0.6	0.0	0.7	0.3	0.0
Maghemite	1.1	1.3	0.4	1.8	0.4	0.4	0.8	1.1	0.1
Hematite	0.7	0.5	0.0	1.3	2.2	0.0	0.4	0.0	0.0
Metakaolin (= glass)	61.0	85.0	85.4	55.1	50.2	68.2	78.1	74.8	86.4

d) Tridymite in task

Power Station No	15	16	17	18	19	20	21	22	23
Quartz	21.6	2.6	7.3	28.3	30.5	12.1	12.7	6.8	6.8
Mullite	22.7	12.2	12.8	17.2	24.3	26.5	13.7	24.5	12.1
Cristobalite	0.0	0.0	0.1	0.1	0.0	0.0	0.1	0.0	0.0
Magnetite	0.8	3.0	0.4	1.8	0.6	0.0	1.2	1.6	0.2
Maghemite	1.4	1.4	0.5	1.9	0.6	0.7	1.0	0.7	0.4
Hematite	1.3	0.8	0.0	1.3	2.5	0.0	0.5	0.0	0.0
Tridymite (= glass)	52.2	80.0	78.8	49.5	41.5	60.7	70.9	66.5	80.4

Table 3: Mineralogy of LTA isolated from feed coals associated with fly ash samples, using X-ray diffraction and Siroquant

Power Station No	16	17	18	19	20	21	23
Coal LTA %	23.3	23.9	13.3	16.8	19.0	27.8	21.7
Quartz	14.3	34.5	37.4	40.8	21.9	28.2	34.3
Kaolinite	63.0	40.6	41.0	48.4	36.6	23.8	31.0
Illite		4.5	8.9	7.9		3.2	0.7
Illite/smectite	12.0	11.1	4.6		39.9	35.3	32.6
Pyrite	1.8		6.2	0.9			0.2
Siderite		2.4		0.1		2.5	0.4
Calcite		1.4				1.9	
Dolomite		1.0				0.7	0.2
Bassanite	7.4	0.6	1.6	1.9	1.0	1.2	0.5
Albite						2.1	
Sanidine		3.4				0.7	
Apatite	1.6					0.5	
Anatase					0.6		
Rutile		0.6	0.3				

A similar plot for the iron minerals in the coal and fly ash (Figure 2b) shows a more scattered but still broadly linear relationship, for five of the samples, between the percentage of iron oxide minerals in the fly ash and the percentage of siderite plus pyrite in the LTA of the corresponding feed coal. This suggests that the iron oxide minerals in the fly ash are derived mainly from the iron minerals present in the coals themselves. However, two fly ashes (circled data points) have high percentages of crystalline iron oxides yet only low percentages of iron minerals in the respective feed coals. The two samples in question are derived from relatively low-rank coals, and the iron minerals in these particular fly ashes may be derived from iron occurring in some other form in the corresponding feed coals, for example in the clay minerals, as amorphous phases, or incorporated into the organic matter.

ESTIMATION OF GLASS COMPOSITION

The chemical composition of the crystalline mineral components in each fly ash was calculated, based on the weight percentages of each mineral as indicated by the respective Siroquant analysis. Although any of the data sets in Table 2 could have been used, the results for the present study were based on the Siroquant data for the ZnO spiked samples. The aggregate percentage of each oxide for the crystalline phases was based on the stoichiometric composition of each mineral identified and the proportion of that mineral as a percentage of the whole ash sample.

The results of this calculation are incorporated into Table 4. These percentages were then subtracted from the bulk chemical composition of the respective ash samples (Figure 3), determined independently by X-ray fluorescence spectrometry, to calculate an inferred chemical composition for the glass fraction (Table 5). Unburnt carbon, although determined separately for the ash samples, was not

included in this calculation, and hence the chemistry of both ash and glass represents a composition normalised to a carbon-free basis.

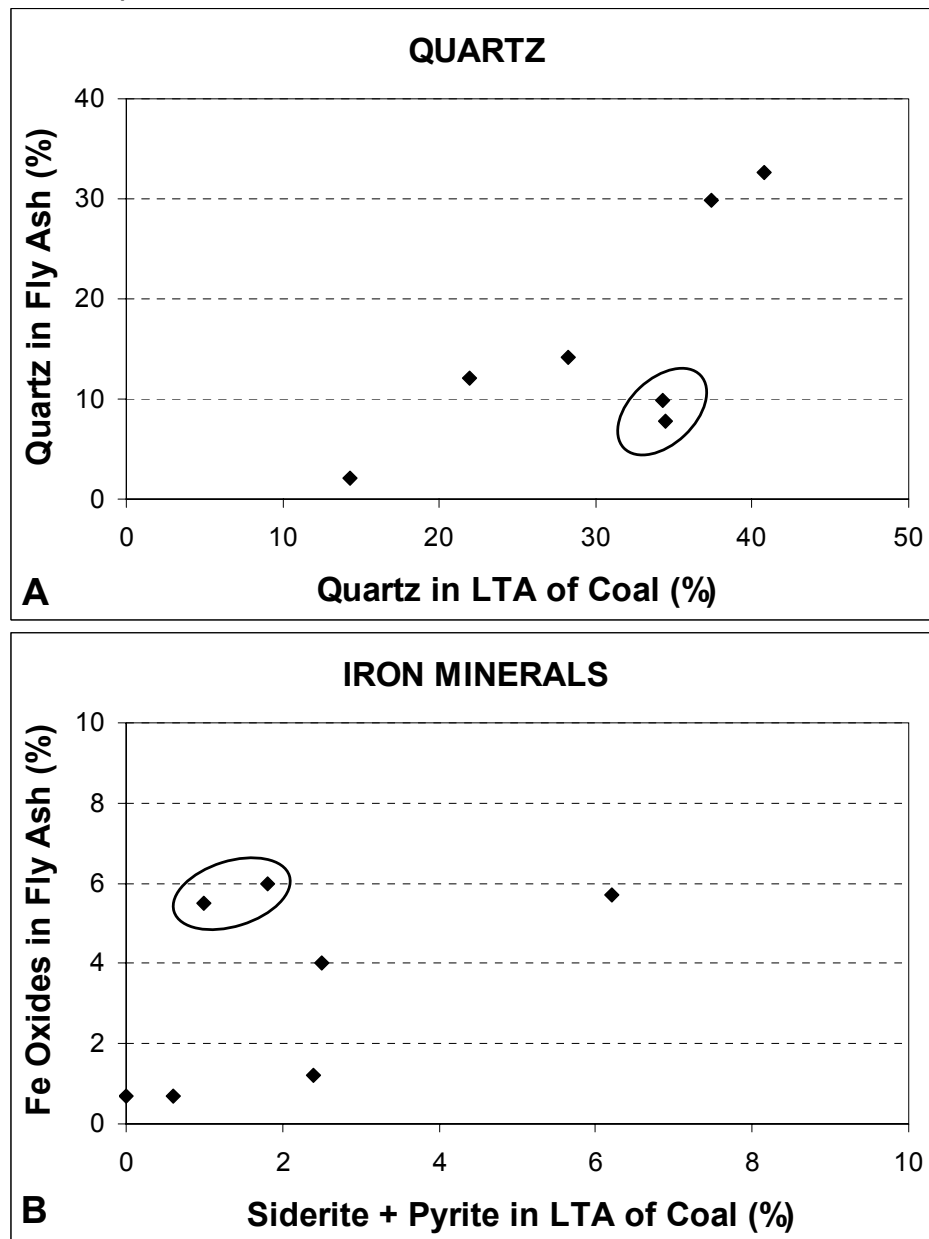


Figure 2: Relation between (A) quartz and (B) iron minerals in fly ashes and in LTA of feed coal samples, as determined by XRD and Siroquant. See text for discussion of circled data points.

Use of stoichiometric compositions for the different minerals possibly represents a slight oversimplification. Gomes and Francois [21], for example, indicate that the mullite in a French fly ash contains slightly more Al_2O_3 and slightly less SiO_2 than the stoichiometric formula. Electron microprobe analyses carried out by the authors of the present paper also show that significant concentrations of iron are often present in the mullite of Australian fly ash. Another study of French fly ash [22] suggests that a small but significant proportion of Mg, along with traces of Mn, Ca and Si, may also occur in the magnetite component, an observation supported by unpublished

data on magnetite compositions for Australian fly ashes, which often contain aluminium in addition to the elements mentioned above. Similar data on mineral chemistry were not available for the fly ashes in the present study, but even so the differences relative to stoichiometric compositions would be expected to be relatively small. They would probably not significantly affect the broader comparisons indicated in the present study.

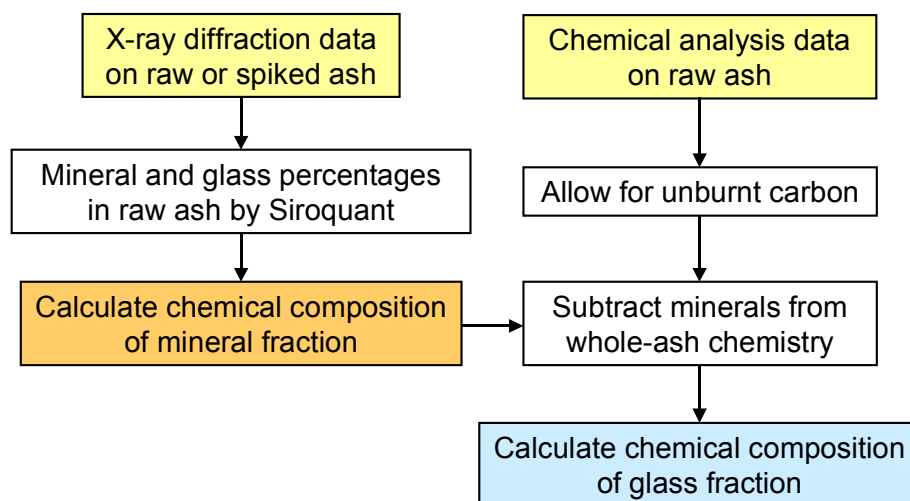


Figure 3: Schematic overview of method for estimating ash composition

VARIATION IN GLASS PERCENTAGE AND COMPOSITION

Based on the glass percentages indicated by Siroquant analysis of the spiked samples, and supported by the data from the raw ashes using tridymite, the percentage of glass in the Australian fly ashes studied ranges from 45 to 80%. The factors controlling this variation probably include the mineralogy and inorganic geochemistry of the original feed coals, as well as the different furnace operating conditions.

The material identified as glass in such studies might also include small proportions of crystalline minerals, at concentrations in the fly ash below the limit of detection by the XRD technique. Possible traces of poorly ordered calcite, for example, have been identified in some diffractograms of the fly ash from Power Station 22. Although difficult to identify positively by XRD, due to problems in discriminating the relevant peaks from the diffractogram background, such phases may also be significant as sites for the occurrence of some of the trace elements in the ash samples.

The inferred glass composition data suggest that the fly ash samples fall into two very distinct groups. One such group (Group A in Table 4) has glass with a relatively low percentage of SiO_2 (45-60%) and a high percentage (more than around 10%) of Fe_2O_3 . The other (Group B) has glass with apparently high SiO_2 (60-70%) and low (typically < 5%) Fe_2O_3 . Although specific details of the respective sites are confidential, the ashes of Group A were derived from coals that are essentially of

sub-bituminous rank, while those of Group B were derived from combustion of bituminous coal feedstocks.

Table 4: Chemical composition of Australian fly ash samples, inferred composition of mineral and glass fractions.

Whole ash chemistry [18], corrected for carbon and LOI

Power Stn No	15	19	18	16	20	17	21	22	23
SiO ₂	56.8	57.0	58.3	44.5	62.9	67.0	61.5	57.5	65.9
Al ₂ O ₃	26.3	25.0	22.2	30.7	29.3	24.8	22.4	28.2	27.6
Fe ₂ O ₃	9.5	9.9	13.6	14.4	1.8	3.1	7.6	5.6	1.1
CaO	1.4	1.5	1.3	4.2	1.3	1.0	3.3	3.8	0.4
BaO	0.4	0.5	0.4	0.1	0.1	0.0	0.1	0.1	0.0
MgO	0.8	0.7	0.8	1.6	1.1	0.6	1.1	1.2	0.3
Na ₂ O	0.2	0.2	0.2	0.4	0.8	0.6	0.9	0.2	0.2
K ₂ O	0.7	0.5	0.4	0.9	0.5	1.6	1.9	1.1	2.9
TiO ₂	1.7	1.5	1.7	1.9	1.8	1.0	0.9	1.6	1.3
P ₂ O ₅	1.9	2.7	1.0	1.0	0.1	0.2	0.2	0.5	0.2
SO ₃	0.3	0.5	0.1	0.3	0.2	0.1	0.1	0.2	0.1
Total	100.0	100.0	100.0	100.0	100.0	100.0	100.0	100.0	100.0

Inferred chemistry – minerals

Power Stn No	Group A				Group B				
	15	19	18	16	20	17	21	22	23
Minerals %	52.7	55.0	53.9	20.0	39.0	20.9	33.7	34.0	26.3
SiO ₂	61.3	68.5	65.0	27.8	50.2	53.7	55.1	40.7	54.5
TiO ₂	0.0	0.0	0.0	0.0	0.0	0.0	0.0	0.0	0.0
Al ₂ O ₃	33.0	21.5	24.4	42.7	48.1	40.5	33.0	51.9	42.9
Fe ₂ O ₃	5.7	10.0	10.6	29.5	1.8	5.7	11.9	7.4	2.7
MgO	0.0	0.0	0.0	0.0	0.0	0.0	0.0	0.0	0.0
CaO	0.0	0.0	0.0	0.0	0.0	0.0	0.0	0.0	0.0
Na ₂ O	0.0	0.0	0.0	0.0	0.0	0.0	0.0	0.0	0.0
K ₂ O	0.0	0.0	0.0	0.0	0.0	0.0	0.0	0.0	0.0
P ₂ O ₅	0.0	0.0	0.0	0.0	0.0	0.0	0.0	0.0	0.0
SO ₃	0.0	0.0	0.0	0.0	0.0	0.0	0.0	0.0	0.0
Total	100.0	100.0	100.0	100.0	100.0	100.0	100.0	100.0	100.0

Inferred chemistry – glass

Power Stn No	Group A				Group B				
	15	19	18	16	20	17	21	22	23
Glass %	47.3	45.0	46.1	80.0	61.0	79.1	66.3	66.0	73.7
SiO ₂	52.3	43.8	50.8	48.8	71.1	70.5	64.9	66.2	66.0
TiO ₂	3.7	3.3	3.7	2.4	3.0	1.2	1.4	2.5	1.3
Al ₂ O ₃	19.2	29.5	19.8	27.8	17.4	20.6	17.0	16.0	27.6
Fe ₂ O ₃	13.9	9.8	17.5	10.6	1.8	2.4	5.4	4.7	1.1
MgO	1.6	1.6	1.9	2.0	1.8	0.8	1.7	1.7	0.3
CaO	2.9	3.4	2.8	5.3	2.1	1.2	5.0	5.8	0.4
Na ₂ O	0.4	0.3	0.3	0.4	1.4	0.7	1.3	0.2	0.2
K ₂ O	1.4	1.2	0.9	1.1	0.8	2.1	2.9	1.7	2.9
P ₂ O ₅	3.9	6.0	2.2	1.2	0.2	0.3	0.2	0.7	0.2
SO ₃	0.6	1.1	0.2	0.3	0.3	0.1	0.2	0.4	0.1
Total	100.0	100.0	100.0	100.0	100.0	100.0	100.0	100.0	100.0

Table 5: Other properties of Australian fly ash samples (all except carbon based on data from Killingley et al. [18])

Power Station No.	Group A				Group B				
	15	19	18	16	20	17	21	22	23
Particle density g/cc	2.1	2.1	2.2	2.2	1.7	2.0	1.9	1.8	2.0
Helium density g/cc	n.d.	n.d.	n.d.	2.4	1.9	2.1	2.1	2.1	2.1
BET surface area m ² /g	9.7	8.6	11.2	3.2	3.1	1.7	1.7	2.5	0.9
BET (non- micropore) m ² /g	4.2	3.9	3.4	2.0	2.0	1.1	1.0	1.5	0.6
Unburnt carbon %	2.17	3.29	2.25	4.71	3.67	1.45	2.65	3.55	0.60

Group A ashes also tend to have higher particle densities (> 2.0) and larger surface areas compared to Group B materials (Table 3). The density values are highest for three of the Group A ashes that also contain abundant iron minerals (magnetite, hematite etc). However, the remaining Group A ash has a lesser proportion of iron minerals but a higher particle density than one of the lower-density Group B ash samples with a relatively high iron mineral content. Glass composition may therefore play a role in determining particle density among these ash samples. The surface area may also be related to the glass composition. Although there is one sample in each group with overlapping values, the Group A ashes tend to have significantly higher surface areas than the Group B ashes. Unburnt carbon, which might separately affect density and surface area, is more or less evenly distributed between both ash groups.

CONCLUSIONS

Rietveld-based X-ray diffraction analysis allows the proportions of both the different minerals and the glass within a fly ash to be evaluated directly in quantitative terms. Analysis can be carried out using an ash sample spiked with a known proportion of a separate mineral, such as corundum or ZnO, without the need for an accompanying series of calibration experiments such as used in other types of XRD study. Alternatively, quantitative estimates of crystalline and glass phases can be made from a powder diffractogram of the raw (unspiked) ash sample, using a low-crystallinity silicate mineral such as metakaolin or tridymite in the Rietveld processing to represent the glass component.

Although the proportions of the different minerals (quartz, mullite, hematite, magnetite etc) vary to a significant extent, the crystalline quartz content and the proportions of iron minerals in the fly ashes also suggest relations to the abundance of particular minerals in the parent coal samples. The composition of the glass fractions also apparently varies with the rank of the coal that dominated the original fuel source. The glass composition also appears to be related to variations in several other ash properties, such as particle density and surface area, which may be significant to different ash utilisation processes.

ACKNOWLEDGEMENTS

The authors wish to acknowledge the financial support provided by the Co-operative Research Centre for Coal in Sustainable Development, which is funded in part by the Cooperative Research Centres Program of the Commonwealth Government of Australia. Funding for other aspects of the work was provided by the Australian Coal Association Research Program (ACARP) under ACARP Project C8051. Thanks are also expressed to a number of power station operators for provision of fly ash samples for analysis, and to Irene Wainwright and Zhongsheng Li for assistance with the analysis program.

REFERENCES

1. Taylor, G.H., Teichmuller, M., Davis, A., Diessel, C.F.K., Littke, R., Robert, P., 1998. *Organic Petrology*. Gebruder Borntraeger, Berlin, 704 pp
2. Hower, J.C., Rathbone, R.F., Robertson, J.D., Peterson, G., Trimble, A.S., 1999. Petrology, mineralogy and chemistry of magnetically-separated sized fly ash. *Fuel*, 78, 197-203.
3. Foner, H.A., Robl, T.L., Hower, J.C., Graham, U.M., 1999. Characterisation of fly ash from Israel with reference to its possible utilisation. *Fuel*, 78, 215-223.
4. Hower, J.C., Mastalerz, M., 2001. An approach toward a combined scheme for the petrographic classification of fly ash. *Energy and Fuels*, 15, 1319-1321.
5. Jenkins, R., Snyder, R.L., 1996. *Introduction to X-ray Powder Diffractometry*. J. Wiley and Sons, New York, 403 pp.
6. Klug, H.P., Alexander, L.E., 1974, *X-Ray Diffraction Procedures*, 2nd Edition: New York, John Wiley and Sons, 656 pp.
7. McCarthy, G.J., Johansen, D.M., 1988. X-ray powder diffraction study of NBS fly ash reference materials. *Powder Diffraction*, 3, 156-161.
8. Seung, H.L., Sakai, E., Daimon, M., Wan, K.B., 1999. Characterisation of fly ash directly collected from electrostatic precipitator. *Cement and Concrete Research*, 29, 1791-1797.
9. Rietveld, H.M., 1969. A profile refinement method for nuclear and magnetic structures. *Journal of Applied Crystallography*, 2, 65-71.
10. Taylor, J.C., 1991. Computer programs for standardless quantitative analysis of minerals using the full powder diffraction profile. *Powder Diffraction*, 6, 2-9.
11. Ward, C.R., Taylor, J.C., Cohen, D.R., 1999b. Quantitative mineralogy of sandstones by X-ray diffractometry and normative analysis. *Journal of Sedimentary Research*, 69, 1050-1062.

12. Taylor, J.C., Zhu, R., 1992, Simultaneous use of observed and calculated standard profiles in quantitative XRD analysis of minerals by the multiphase Rietveld method – the determination of pseudorutile in mineral sands products. *Powder Diffraction*, 7, 152-161.
13. Taylor, J.C., Matulis, C.E., 1994, A new method for Rietveld clay analysis: Part 1 – use of a universal measured standard profile for Rietveld quantification of montmorillonites. *Powder Diffraction*, 9, 119-123.
14. Ward, C.R., Spears, D.A., Booth, C.A., Staton, I., Gurba, L.W., 1999a. Mineral matter and trace elements in coals of the Gunnedah Basin, New South Wales, Australia. *International Journal of Coal Geology*, 40, 281-308.
15. Ward, C.R., Matulis, C.E., Taylor, J.C., Dale, L.S., 2001. Quantification of mineral matter in the Argonne Premium Coals using interactive Rietveld-based X-ray diffraction. *International Journal of Coal Geology*, 46, 67-82.
16. Ward, C.R., 2001. Quantitative mineralogical analysis of coal and associated materials by X-ray diffractometry. *Proceedings of 18th International Pittsburgh Coal Conference, Newcastle, NSW, 18 pp. (CD-ROM)*
17. Ruan, C.D., Ward, C.R., 2002. Quantitative X-ray powder diffraction analysis of clay minerals in Australian coals using Rietveld methods. *Applied Clay Science*, 21, 227-240.
18. Killingley, J., McEvoy, S., Dokumcu, C., Stauber, J., Dale, L., 2000. Trace element leaching from fly ash from Australian Power Stations. End of Grant Report, Australian Coal Association Research Program, Project C8051, CSIRO Division of Energy Technology.
19. Winburn, R.S., Grier, D.G., McCarthy, G.J., Peterson, R.B., 2000. Rietveld quantitative X-ray diffraction analysis of NIST fly ash standard reference materials. *Powder Diffraction*, 15, 163-172.
20. Gluskoter, H.J., 1965. Electronic low temperature ashing of bituminous coal. *Fuel* 44, 285-291.
21. Gomes, S., Francois, M., 2000. Characterisation of mullite in silicoaluminous fly ash by XRD, TEM and ²⁹Si MAS NMR. *Cement and Concrete Research*, 30, 175-181.
22. Gomes, S., Francois, M., Abdelmoula, M., Refait, P., Pellissier, C., Evrard, O., 1999. Characterisation of magnetite in silico-aluminous fly ash by SEM, TEM, XRD, magnetic susceptibility and Mössbauer spectroscopy. *Cement and Concrete Research*, 29, 1705-1711.